

Table S1 Contributing weather stations ($n=6$) to the PRISM 4K (T_{mean} and T_{max}) gridded data field proximal to the three study sites. All stations are located between 37.0–35.9 °N and 105.8–104.4 °W.

| | Latitude (°N) | Longitude (°W) | Elevation (m) | Years | Terrain |
|-------------------|---------------|----------------|---------------|-----------|-----------------------------------|
| Cimarron 4 SW | 36.47 | 104.95 | 2071 | 1904–2019 | Hilly, Warm grass/shrub |
| Red River | 36.71 | 105.40 | 2981 | 1906–2015 | Mountain valley, Cool conifer |
| Springer | 36.36 | 104.58 | 1784 | 1891–2014 | Hilly, Warm grass/shrub |
| Raton/Crews Field | 36.75 | 104.75 | 1966 | 1948–1968 | Mountain valley, Warm grass/shrub |
| Manassa | 37.17 | 105.94 | 2354 | 1893–2014 | Mountain valley, Warm grass/shrub |
| Trinidad | 37.18 | 104.49 | 2016 | 1899–2019 | Mountain valley, Cool irrigated |

Table S2 Correlation matrix for all ring-width (RW), latewood blue intensity (LWB), Delta BI (Δ BI), and maximum latewood density (MXD) records developed from Engelmann spruce at the Wheeler Peak (WHE), Serpent Lake (JIS), and San Leonardo Lakes (SLE) sites in the Sangre de Cristo Mountains, northern NM. Bold coefficients denote $p<0.001$. See Table 1 for lengths of records.

| | WHE.RW | WHE.EWB | WHE.LWB | WHE. Δ BI | WHE.MXD | JIS.RW | JIS.EWB | JIS.LWB | JIS. Δ BI | SLE.RW | SLE.EWB | SLE.LWB | SLE. Δ BI |
|------------------|-------------|-------------|-------------|------------------|-------------|-------------|-------------|-------------|------------------|-------------|-------------|-------------|------------------|
| WHE.RW | - | -0.02 | 0.20 | 0.32 | 0.11 | 0.45 | -0.15 | 0.12 | 0.27 | 0.41 | -0.07 | 0.10 | 0.18 |
| WHE.EWB | -0.02 | - | 0.76 | 0.51 | 0.37 | -0.02 | 0.43 | 0.53 | 0.39 | 0.05 | 0.58 | 0.62 | 0.42 |
| WHE.LWB | 0.20 | 0.76 | - | 0.92 | 0.48 | 0.11 | 0.29 | 0.65 | 0.64 | 0.10 | 0.40 | 0.64 | 0.60 |
| WHE. Δ BI | 0.32 | 0.51 | 0.92 | - | 0.48 | 0.18 | 0.16 | 0.62 | 0.71 | 0.17 | 0.24 | 0.54 | 0.61 |
| WHE.MXD | 0.11 | 0.37 | 0.48 | 0.48 | - | 0.34 | 0.17 | 0.41 | 0.57 | 0.30 | 0.20 | 0.40 | 0.47 |
| JIS.RW | 0.45 | -0.02 | 0.11 | 0.18 | 0.34 | - | 0.12 | 0.42 | 0.59 | 0.71 | -0.24 | 0.40 | 0.40 |
| JIS.EWB | -0.15 | 0.43 | 0.29 | 0.16 | 0.17 | 0.12 | - | 0.73 | 0.31 | 0.14 | 0.28 | 0.28 | 0.33 |
| JIS.LWB | 0.12 | 0.53 | 0.65 | 0.65 | 0.41 | 0.42 | 0.73 | - | 0.84 | 0.36 | 0.20 | 0.52 | 0.67 |
| JIS. Δ BI | 0.27 | 0.39 | 0.64 | 0.71 | 0.57 | 0.59 | 0.31 | 0.84 | - | 0.49 | 0.05 | 0.44 | 0.70 |
| SLE.RW | 0.41 | 0.05 | 0.10 | 0.17 | 0.30 | 0.71 | 0.14 | 0.36 | 0.49 | - | -0.02 | 0.31 | 0.59 |
| SLE.EWB | -0.07 | 0.58 | 0.40 | 0.24 | 0.20 | -0.24 | 0.17 | 0.20 | 0.05 | -0.02 | - | 0.80 | 0.35 |
| SLE.LWB | 0.10 | 0.62 | 0.64 | 0.64 | 0.40 | 0.40 | 0.28 | 0.52 | 0.44 | 0.31 | 0.80 | - | 0.77 |
| SLE. Δ BI | 0.27 | 0.46 | 0.60 | 0.61 | 0.47 | 0.40 | 0.33 | 0.67 | 0.70 | 0.59 | 0.33 | 0.77 | - |

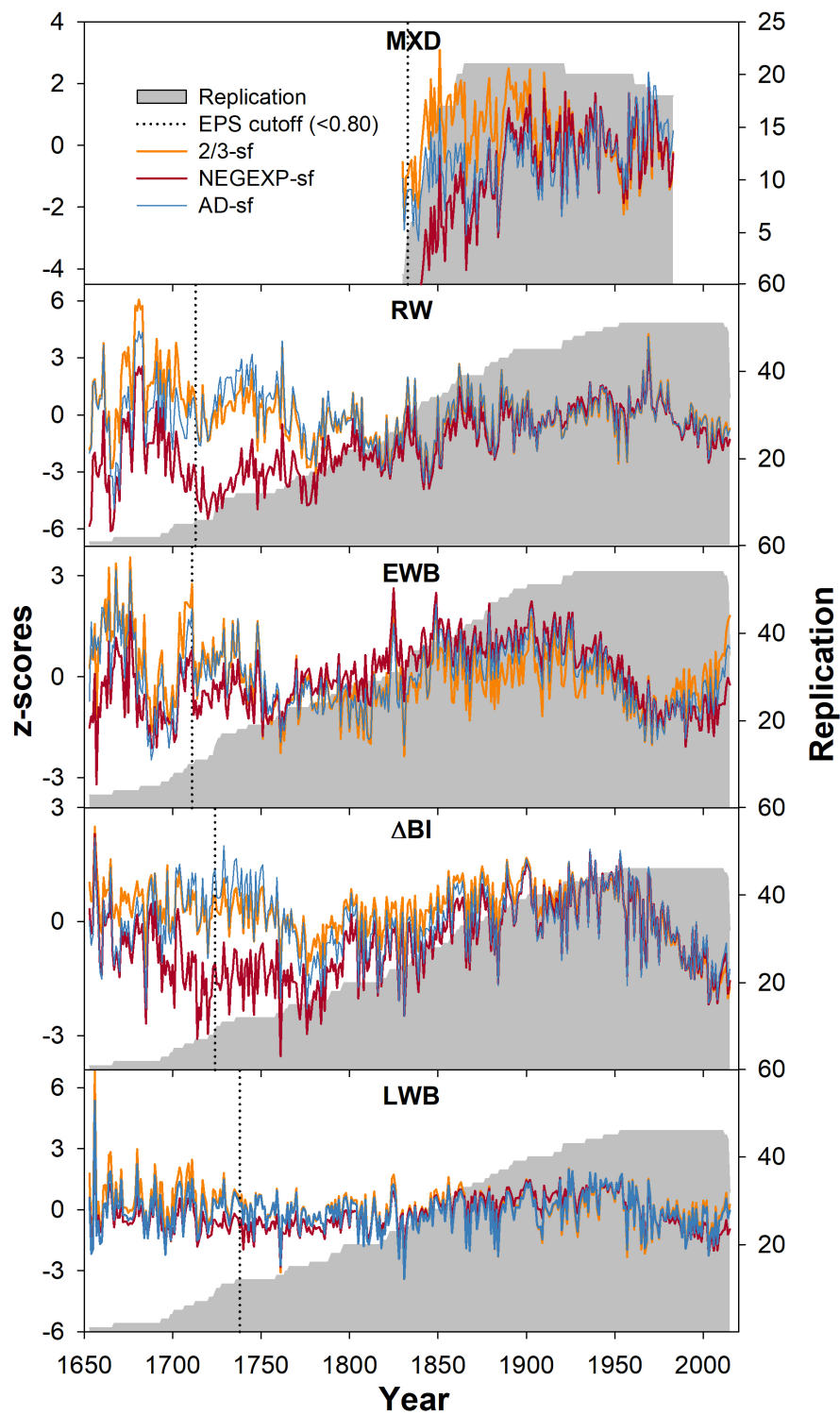


Fig. S1 WHE maximum latewood density (MXD), composite ring-width (RW), earlywood blue intensity (EWB), delta blue intensity (Δ BI), and latewood blue intensity (LWB) chronology variants, EPS, and replication. Composite chronologies derived from PCA of pooled series from WHE, JIS, and SLE. Differential chronology variants for each tree ring parameter result from detrending with the $\frac{2}{3}$ spline in SignalFree ($\frac{2}{3}$ sf, red line), the Age-dependent spline in SignalFree (AD-sf, blue line), and the Negative Exponential spline in SignalFree (NegExp-sf, orange line). EPS determination based on tree ring chronology developed with AD-sf detrending.

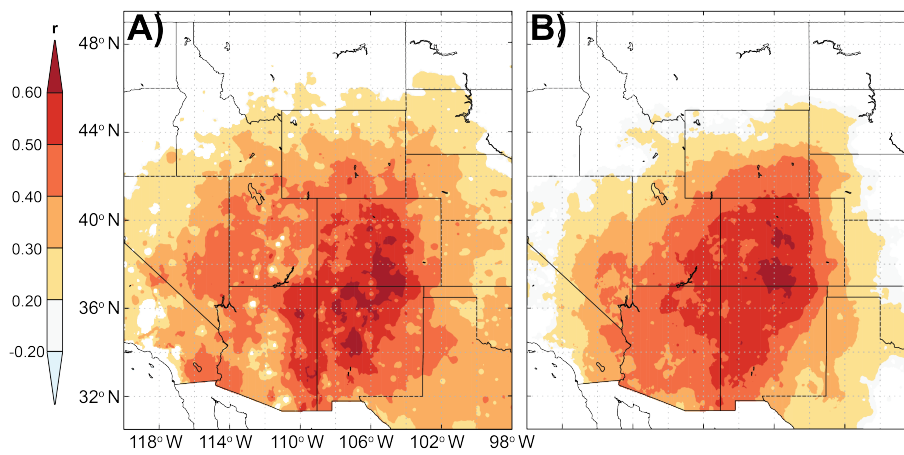


Fig. S2 Spatial correlations ($\alpha=0.10$) across the Southern Rocky Mountains/American Southwest regions between the (A) non-transformed and (B) first year difference composite AD-sf LWB chronology and regional PRISM 4k AS T_{max} over the period 1907–2015.

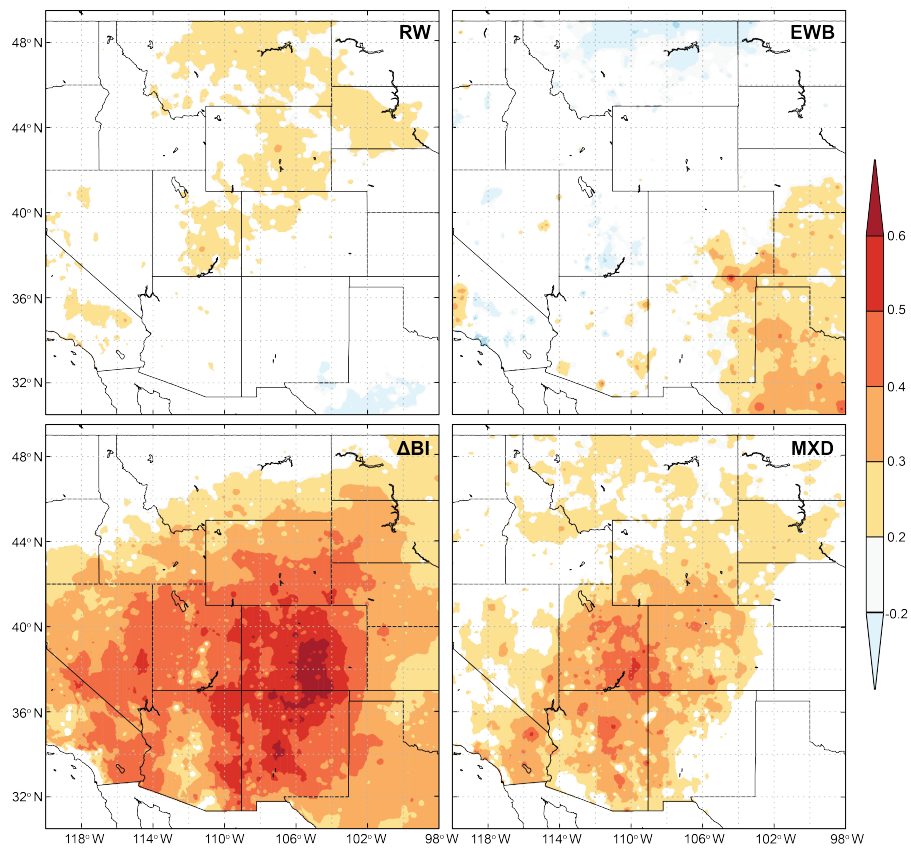


Fig. S3 Spatial correlations ($\alpha=0.10$) across the Southern Rocky Mountains between composite RW, EWB, and Δ BI chronologies and regional PRISM 4k AS T_{max} over the period 1907–2015, and between WHE MXD chronology regional PRISM 4k AS T_{max} over the period 1907–1983.

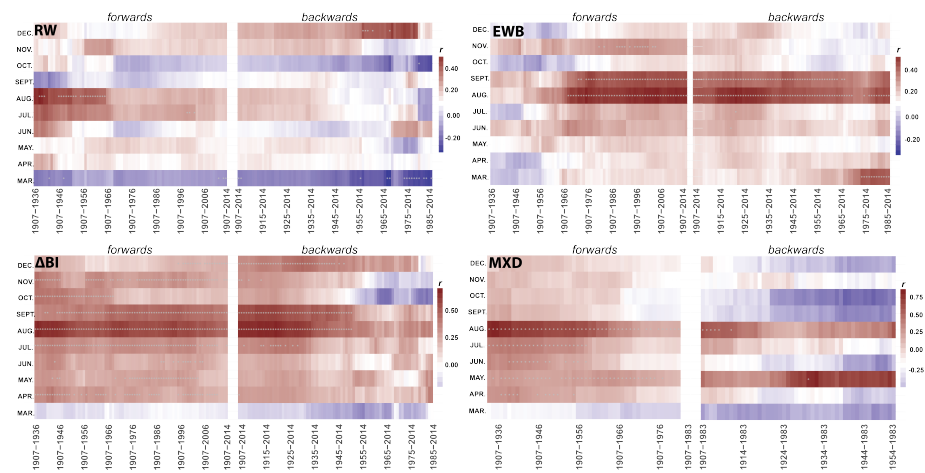


Fig. S4 Forward and backward (evolutionary) moving correlation ($\alpha=0.05$) of composite RW, LWB, and ΔBI chronologies and regional PRISM 4k AS T_{max} over the period 1907–2014, and between WHE MXD chronology regional PRISM 4k AS T_{max} over the period 1907–1983. Note differential color scales for correlation coefficient (r) between parameters.

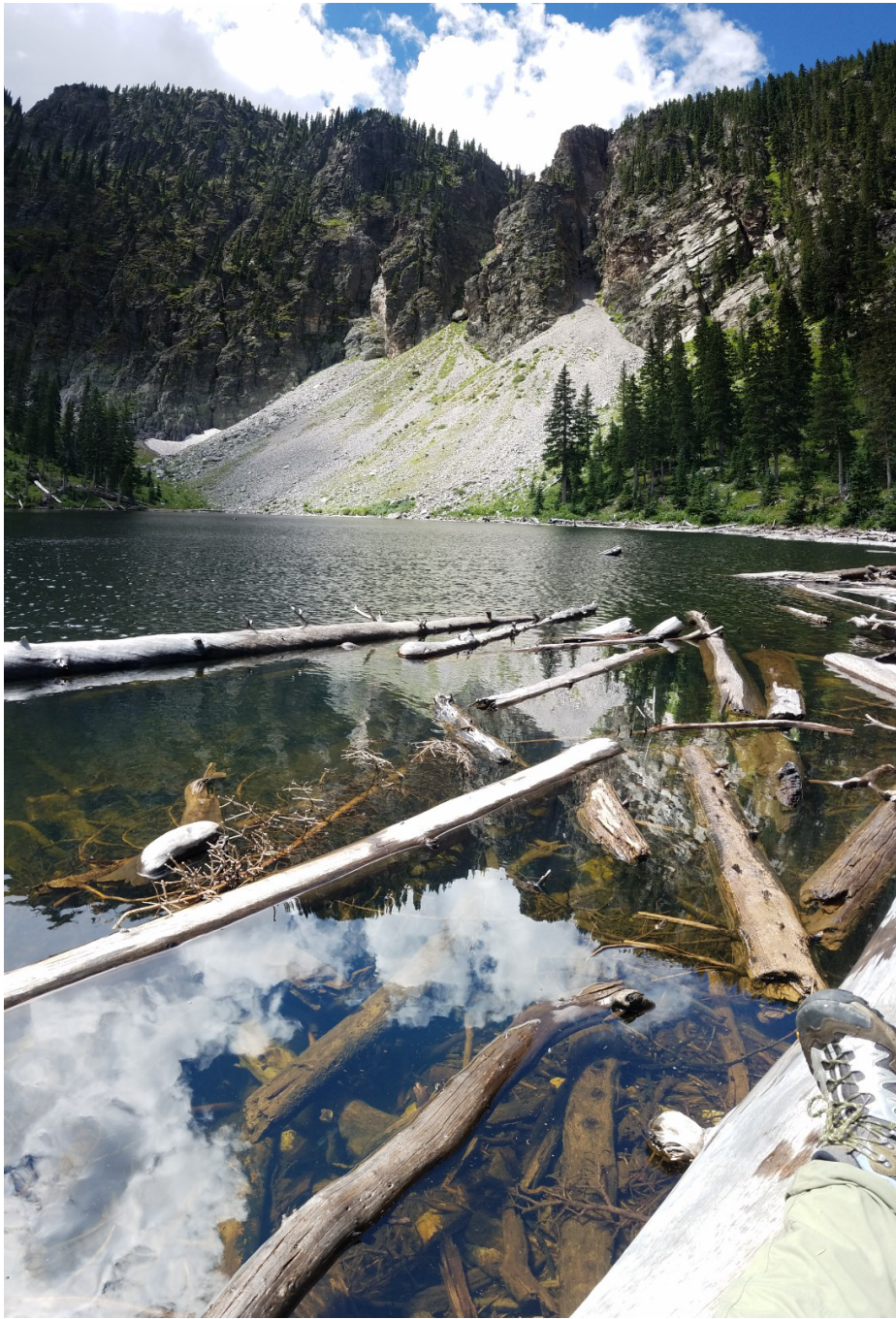


Fig. S5 Photograph of Upper San Leonardo Lake, Sangre de Cristo Mountains, northern NM showing abundance of floating and submerged Engelmann spruce logs.

Table S3 Summary statistics (r values) for individual PCAs (RW, LWB, and Δ BI) of all series from WHE, JIS, and SLE and loadings of each site into the first three PCs.

| | % of variance | WHE | JIS | SLE |
|-----------------|---------------|-------|-------|-------|
| RW PC1 | 40.9% | 0.72 | 0.37 | 0.37 |
| EWB PC1 | 30.7% | 0.54 | 0.45 | 0.40 |
| LWB PC1 | 35.5% | 0.62 | 0.44 | 0.48 |
| Δ BI PC1 | 30.8% | 0.61 | 0.44 | 0.35 |
| RW PC2 | 9.6% | 0.05 | 0.16 | 0.27 |
| EWB PC2 | 10.5% | 0.01 | 0.14 | -0.01 |
| LWB PC2 | 11.4% | 0.10 | 0.18 | 0.0 |
| Δ BI PC2 | 10.5% | 0.05 | 0.25 | 0.03 |
| RW PC3 | 7.5% | -0.12 | 0.16 | 0.08 |
| EWB PC3 | 7.0% | 0.03 | 0.02 | 0.03 |
| LWB PC3 | 6.6% | 0.0 | -0.04 | 0.06 |
| Δ BI PC3 | 6.4% | 0.06 | 0.05 | 0.00 |

Table S4 RBAR and EPS statistics. Included metrics are the RBAR, number of series needed to attain an EPS of 0.80, and the year at which EPS is >0.80 threshold for all detrended (AD-sf) composite chronologies.

| | RW | EWB | LWB | Δ BI |
|------------------------|------|------|------|-------------|
| RBAR | 0.33 | 0.24 | 0.29 | 0.28 |
| No. series EPS >0.80 | 6 | 12 | 13 | 9 |
| Year EPS >0.80 | 1713 | 1721 | 1738 | 1724 |

Table S5 Correlation coefficients of composite chronologies with PRISM 4k August–September mean (AS T_{mean}) and maximum (AS T_{max}) temperature, as well as precipitation data proximate to the three sample locations in the Southern Rocky Mountains region of northern NM (37.0–35.9°N, 105.8–104.4°W). **Bold** coefficients = $p < 0.001$

| | RW | EWB | LWB | Δ BI | MXD |
|--------------------------------------|-------------|--------------|--------------|--------------|------|
| T_{mean} (1907–2015) | 0.03 | 0.21 | 0.54 | 0.43 | - |
| T_{max} (1907–2015) | 0.07 | 0.37 | 0.64 | 0.56 | - |
| T_{mean} (1907–1983) | 0.01 | 0.15 | 0.56 | 0.55 | 0.13 |
| T_{max} (1907–1983) | -0.03 | 0.41 | 0.65 | 0.64 | 0.18 |
| Previous Year May Precip (1907–2015) | 0.08 | 0.04 | -0.01 | 0.03 | - |
| Previous Year May Precip (1980–2015) | 0.54 | -0.23 | 0.23 | 0.44 | - |
| Current April–May Precip (1907–2015) | -0.04 | 0.20 | -0.01 | -0.10 | - |
| Current April–May Precip (1980–2015) | 0.06 | -0.16 | -0.09 | 0.02 | - |
| Current August Precip (1907–2015) | 0.01 | -0.30 | -0.40 | -0.31 | - |
| Current August Precip (1980–2015) | 0.15 | -0.54 | -0.46 | -0.14 | - |

Table S6 Cross-validation statistics for the Southern Rocky Mountains composite LWB AS T_{max} reconstruction spanning 1735–2015 CE. To ensure model stability over time, validation statistics are calculated for calibrating on the early period (1907–1961) and verifying on the late period (1962–2015), and vice-versa. CR^2 (VR^2) = calibration (verification) period coefficient of determination; VRE (VCE) = validation period reduction of error (coefficient of efficiency); RMSE = root-mean-square error.

| Validation/Cross-validation | CR^2 | VR^2 | VRE | VCE | RMSE |
|--|--------|--------|------|------|------|
| Early Period Calibration / Late Period Verification | | | | | |
| Calibration (1907–1961) | 0.30 | – | – | – | 0.93 |
| Verification (1962–2015) | – | 0.31 | 0.57 | 0.16 | – |
| Late Period Calibration / Early Period Verification | | | | | |
| Calibration (1962–2015) | 0.31 | – | – | – | 0.96 |
| Verification (1907–1961) | – | 0.30 | 0.61 | 0.22 | – |
| Full Period (1907–2015) | 0.42 | 0.28 | 0.41 | 0.28 | 0.94 |

Table S7 Top five warmest and coolest single-year and decade anomalies based on the composite LWB AS T_{max} reconstruction for the Southern Rocky Mountains spanning 1735–2015.

| Coldest | Years | Anomaly | Decade | Anomaly |
|---------|-------|---------|-----------|---------|
| 1 | 1831 | -3.64 | 1990–1999 | -1.04 |
| 2 | 1761 | -2.28 | 1810–1819 | -0.98 |
| 3 | 1828 | -2.58 | 1830–1839 | -0.96 |
| 4 | 1884 | -2.49 | 2000–2009 | -0.93 |
| 5 | 2003 | -2.47 | 1760–1769 | -0.28 |
| Warmest | Years | Anomaly | Decade | Anomaly |
| 1 | 1924 | +2.15 | 1940–1949 | +1.05 |
| 2 | 1926 | +2.05 | 1930–1939 | +0.88 |
| 3 | 2015 | +1.99 | 1950–1959 | +0.62 |
| 4 | 1936 | +1.95 | 1890–1899 | +0.34 |
| 5 | 1939 | +2.47 | 1910–1919 | +0.33 |